Organozinc Compounds as Effective Dielectric Modification Layers for Polymer Field-Effect Transistors

Xinjun Xu, Bo Liu, Yingping Zou, Yunlong Guo, Lidong Li, and Yunqi Liu**

The interface between the organic semiconductor and dielectric plays an important role in determining the device performance of organic field-effect transistors (OFETs). Although self-assembled monolayers (SAMs) made from organosilanes have been widely used for dielectric modification to improve the device performance of OFETs, they suffer from incontinuous and lack uniform coverage of the dielectric layer. Here, it is reported that by introduction of a solution-processed organozinc compound as a dielectric modification layer between the dielectric and the silane SAM, improved surface morphology and reduced surface polarity can be achieved. The organozinc compound originates from the reaction between diethylzinc and the cyclohexanone solvent, which leads to formation of zinc carboxylates. Being annealed at different temperatures, organozinc compound exists in various forms in the solid films. With organozinc modification, p-type polymer FETs show a high charge carrier mobility that is about two-fold larger than a control device that does not contain the organozinc compound, both for devices with a positive threshold voltage and for those with a negative one. After organozinc compound modification, the threshold voltage of polymer FETs can either be altered to approach zero or remain unchanged depending on positive or negative threshold voltage they have.

1. Introduction

Organic field-effect transistors (OFETs) have received considerable attention in the past decades due to their potential applications in large-area, low-cost, flexible and printed electronics such as radio frequency identification tags, smart cards, sensors, and organic active matrix displays.[1–4] A typical OFET is composed of a gate electrode, a gate dielectric layer, an organic semiconductor layer and source-drain electrodes. Charge carrier mobility (μ) is one of the most important parameters for evaluating the device performance of OFETs.[5] It is well known that the transport of charge carriers in OFET is extremely restricted by the first several semiconductor monolayers next to the semiconductor–insulator interface.[6,7] Thus, the dielectric–semiconductor interface plays an important role in the charge transport in OFETs. For these reasons, particular attention is focused on the semiconductor–insulator interface to find the nature at this narrow region for improving performance of OFETs.[8–11]

Although the nature of interfacial effects between the semiconductor and dielectric in OFETs is still under debate currently, several interfacial factors have already been described as causations to vary performances of OFETs. The surface roughness, surface energy, surface polarity and dielectric constant of the dielectric layer are considered as important parameters at the semiconductor–insulator interface and have been discussed widely. The commonly used dielectric materials in OFETs are silicon oxide (SiO_2) and metal oxides such as Al_2O_3, TiO_2, and hafnium oxide. In most cases, dielectric modification, which means surface modification of the gate insulator, is necessary either to lower/match the surface energy or to reduce the trap sites at the semiconductor-insulator interface. For such a purpose, self-assembled monolayers (SAMs) made from organosilane compounds and organophosphonates have been introduced through chemical bonding to the surface hydroxyl groups of the dielectric layer in OFETs.[12–15] Alternatively, insulating polymers such as polystyrene, poly(methyl methacrylate) (PMMA), and poly(N-vinylpyrrolidone) (PVP) can also be used as a dielectric modification layer. However, these polymers can be easily solved in commonly-used organic solvents, so they are not suitable for conjugated polymer based OFETs and inkjet-printed OFETs which employ organic solvent for deposition of the active film layer. To solve this problem, cross-linked materials such as divinyltetramethylsiloxane-bis(benzocyclobutene) derivative (BCB),[16,17] Cytop,[18] poly(methyl silsesquioxane) (PMSQ)[19,20] have been developed to serve as a dielectric modification layer. Nevertheless, these cross-linked polymers are usually amorphous which may introduce additional carrier trapping sites at the dielectric-semiconductor interface.

Dr. X. Xu, Prof. L. Li
State Key Lab for Advanced Metal and Materials
School of Materials Science and Engineering
University of Science and Technology Beijing
Beijing 100083, P. R. China
E-mail: lidong@mater.ustb.edu.cn
B. Liu, Prof. Y. Zou
College of Chemistry and Chemical Engineering
Central South University
Changsha 410083, P. R. China
Dr. Y. Guo, Prof. Y. Liu
National Laboratory for Molecular Sciences
Institute of Chemistry
Chinese Academy of Sciences
Beijing 100190, P. R. China
E-mail: liuyq@iccas.ac.cn

DOI: 10.1002/adfm.201200316

In contrast, as for the SAMs modification layer mentioned above, crystalline SAMs of organosilane compounds such as octadecyltrimethoxysilane (OTMS) and octadecyltrichlorosilane (OTCS) can be formed given that appropriate deposition methods were adopted.[12,13,21] OFETs based on crystalline SAM modified dielectric layer showed several-fold increase in hole mobility and more than one order of magnitude increase in electron mobility compared with devices with amorphous SAM modified surfaces.[12,13] So, up to now, SAM-based dielectric modification is still an very effective way to improve the OFET performance. However, additional problems remain. All the reported SAM-based dielectric modifications require active surface functional groups be present to permit chemical reaction with the modification agents to result in chemical bonding on the surface. For example, surface hydroxy groups are needed for SAM modification in the case of SiO_2 surface with alkyltrichlorosilane. Such surface hydroxy groups are generally introduced through hydrophilic treatment of the substrates. As a result, the quality of SAMs, which are critically dependent on the nature of surface functional groups, can profoundly influence the final device performance. It has been shown that coverage of dielectric surface by alkylsilane SAMs are usually not uniform even in the case of crystalline SAMs.[12] Therefore, if a suitable dielectric modification material which facilitates the chemical bonding of alkylsilanes to its surface can be found, the above-mentioned drawbacks will be overcome.

Diethylzinc (DEZn), a reactive compound, has usually been used as an efficient catalyst in organic reactions such as epoxide polymerization,[22,23] reduction of aldehydes and ketones,[24,25] and as reactants for conjugate addition reactions.[26] In addition, doping magnetic nanoparticles and semiconductor nanowires by DEZn to adjust their properties have also been reported.[27–29] Recently, DEZn has been employed as a starting material for forming electron acceptors in bulk-heterojunction organic solar cells.[30–32] However, utilization of DEZn in OFETs has never been reported. In this paper, we demonstrate that DEZn can be transformed to a zinc carboxylate compound in a solution-deposited film which serves as an effective dielectric modification layer in OFETs. By using this kind of dielectric modification layer, the quality of SAM on the dielectric surface can be improved, leading to enhanced charge carrier mobility in OFET.

2. Results and Discussion

It has been reported that DEZn can be converted to zinc oxide (ZnO) using toluene and tetrahydrofuran (THF) as solvents for film deposition.[30] However, the circumstance is changed when cyclohexanone is employed as the solvent. **Figure 1**a shows the ultraviolet-visible (UV-vis) absorption spectra of solid films deposited from the cyclohexanone solution of DEZn (denoted as organozinc films throughout this paper), which were annealed at 180 °C, 120°C, 90 °C, and room temperature (RT), respectively. Such films exhibit similar absorption spectra and only show a very weak absorption peak around 245 nm, which differs from that of ZnO nanoparticles (whose absorption peak lies between 300–375 nm).[33] With increasing the annealing temperature, the peak at 245 nm becomes weaker and weaker.

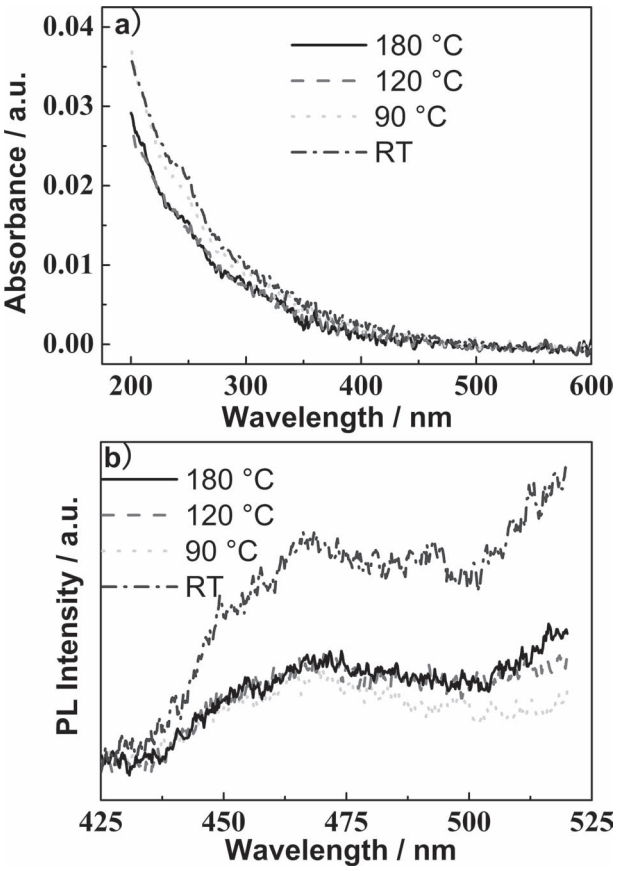

Figure 1. a) UV-vis absorption and b) PL emission spectra of organozinc films annealed at different temperatures. For the PL measurement, the excitation wavelength is 280 nm.

Figure 1b shows the corresponding photoluminescence (PL) spectra of these organozinc films. It can be seen these films have a weak peak at 468 nm and a shoulder at 451 nm. We didn't observe any detectable emission with wavelength under 420 nm (not included in the spectra), which means the films are not composed of ZnO since ZnO has a characteristic band-edge emission around 380 nm.[34] The weak emission peak at 468 and 451 nm might be attributed to the recombination of a photogenerated hole with a charge state of a specific defect such as vacancies or the surface deep traps.[34,35]

Figure 2 shows the X-ray diffraction (XRD) patterns of the organozinc films annealed at various temperatures. In addition, to tune the surface properties, the 180 °C-annealed organozinc film was modified with a SAM composed of OTMS similar as the way reported by Ito et al. for depositing SAMs of OTMS on the surface of SiO_2.[12] The XRD pattern of the SAM modified organozinc compound is also shown in Figure 2. A broad peak can be seen in all these films with 2θ value around 33–34° corresponding to the amorphous states in the organozinc film. With increasing the annealing temperature to 120 °C, a sharp and narrow crystalline peak occurred at 32.8°. This crystalline peak becomes more intense at high annealing temperature of 180 °C. This can be attributed to more crystalline states being formed in the film annealed at higher temperatures. After SAM

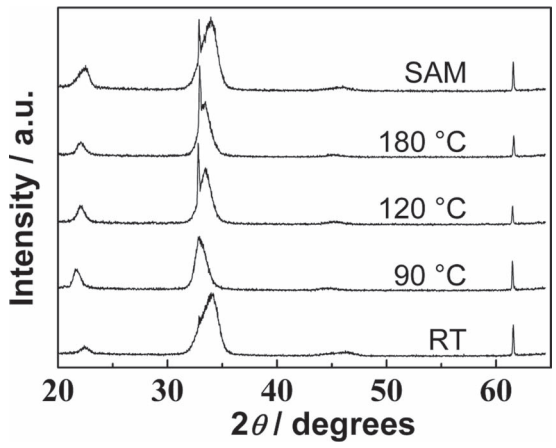

Figure 2. XRD of organozinc films annealed at different temperatures. SAM stands for modification of the 180 °C-annealed organozinc film with OTMS.

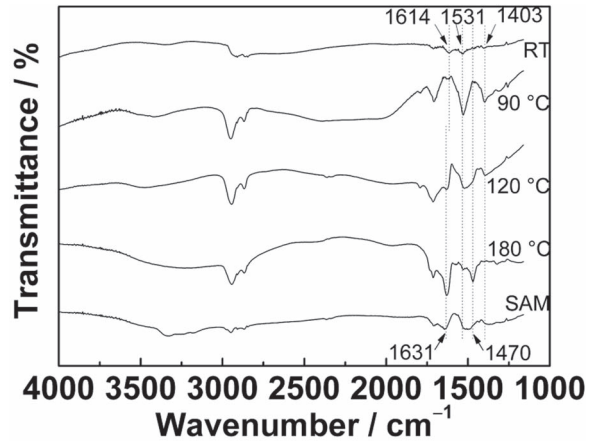

Figure 3. IR spectra of organozinc films annealed at different temperatures. SAM stands for modification of the 180 °C-annealed organozinc film with OTMS. The dotted line is a guide to the eye.

modification, the organozinc film shows a weakened peak at 32.8°. Other peaks seem almost unchanged after annealing at different temperatures.

Figure 3 shows the infrared (IR) transmittance spectra of the annealed organozinc films and SAM-modified organozinc film. The spectrum of the film annealed at RT exhibits peaks at 2950 and 2870 cm^{-1} correspond to CH_2 asymmetrical and symmetrical stretching bands, respectively. Moreover, it shows observable absorption peaks at 1614, 1531 cm^{-1} and a weak one at 1403 cm^{-1} corresponding to the characteristic peaks of coordinated carboxylate groups. These three peaks can be assigned to two asymmetric carboxylate stretching modes (ν_{as} = 1614 and 1531 cm^{-1}) and one symmetric carboxylate stretching mode (ν_s = 1403 cm^{-1}) of carboxylate groups.[36] A common structure for zinc carboxylates is that in which two zinc atoms are linked by three *syn-syn* bridging carboxylate ligands to form a binuclear unit $[Zn_2(OOCR)_3]^+$, where R stands for alkyl or aryl. These units are linked to one another by a *syn-anti* bridging carboxylate ligand to produce a linear (3,l) polymer (see **Scheme 1**).[36] In some cases, a chain of zinc atoms is linked by pairs of *syn-syn* bridging carboxylate ligands to give a (2,2) bridged polymer structure.[37] For the linear (3,1) polymer of zinc carboxylate, the solid-state IR spectra exhibit two ν_{as} modes due to the presence of two kinds of bridging carboxylate ligand i.e. *syn-syn* and *syn-anti*. However, for the linear (2,2) polymer, there is only one ν_{as} mode since it contains *syn-syn* bridging modes only. As there are two ν_{as} modes (1614 and 1531 cm^{-1}) found in our case, we can deduce that the structure of organozinc compound in RT annealed film is a (3,1) chain polymer of zinc carboxylate. The spectrum of the film annealed at 90 °C shows enhanced intensities at 1531 (ν_{as} in the *syn-syn* bridging mode) and 1403 cm^{-1} (ν_s mode), but a reduced one at 1614 cm^{-1} (ν_{as} in the *syn-anti* bridging mode) compared with the film annealed at RT. The peak at 1712 cm^{-1} and the very broad peak centered at 3419 cm^{-1} can be assigned to the C = O stretching in hydrogen bonded carboxyl acid dimers and the associated (hydrogen bonded) hydroxyl groups, respectively.[38,39] With increasing the annealing temperature to 120 °C, the organozinc film shows an additional peak located at 1631 cm^{-1} and a shoulder at 1470 cm^{-1} next to the peak of 1531 cm^{-1}. As for the 180 °C annealed organozinc film, the peaks at 1631 and 1470 cm^{-1} become dominant. Meanwhile, $\nu_{as}(COO^-)$ (1531 cm^{-1}) and $\nu_s(COO^-)$ (1403 cm^{-1}) of the *syn-syn* bridged carboxylate groups become very weak. Some reports have shown that zinc oxocarboxylates ($Zn_4O(OOCR)_6$, R = alkyl or aryl) can be formed when zinc carboxylates were treated in a hot ketone solution.[36,40] The $Zn_4O(O_2CR)_6$ complex possesses a central O atom, which is surrounded by four Zn atoms in a perfect tetrahedral coordination. The six edges of the Zn_4 tetrahedron are bridged by carboxylate groups. The reported zinc oxocarboxylate exhibits $\nu_{as}(COO^-)$ at 1639 cm^{-1} and $\nu_s(COO^-)$

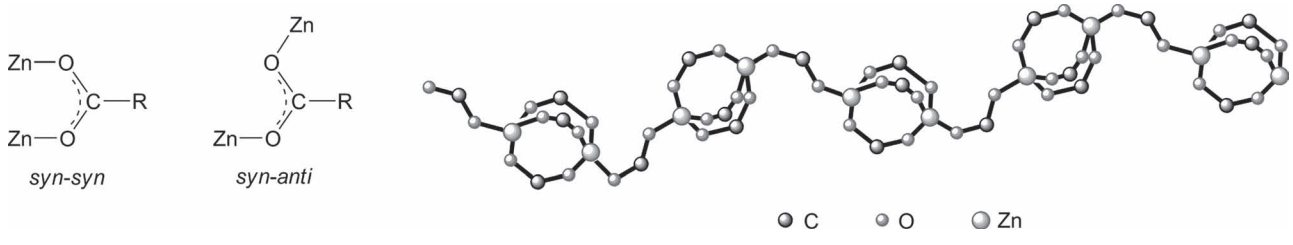

Scheme 1. Zinc carboxylates with a *syn-syn* (left) and *syn-anti* (middle) bidentate bridge, and in the (3,1) chain polymer form (right). Side chains of carboxylate ligands not shown.

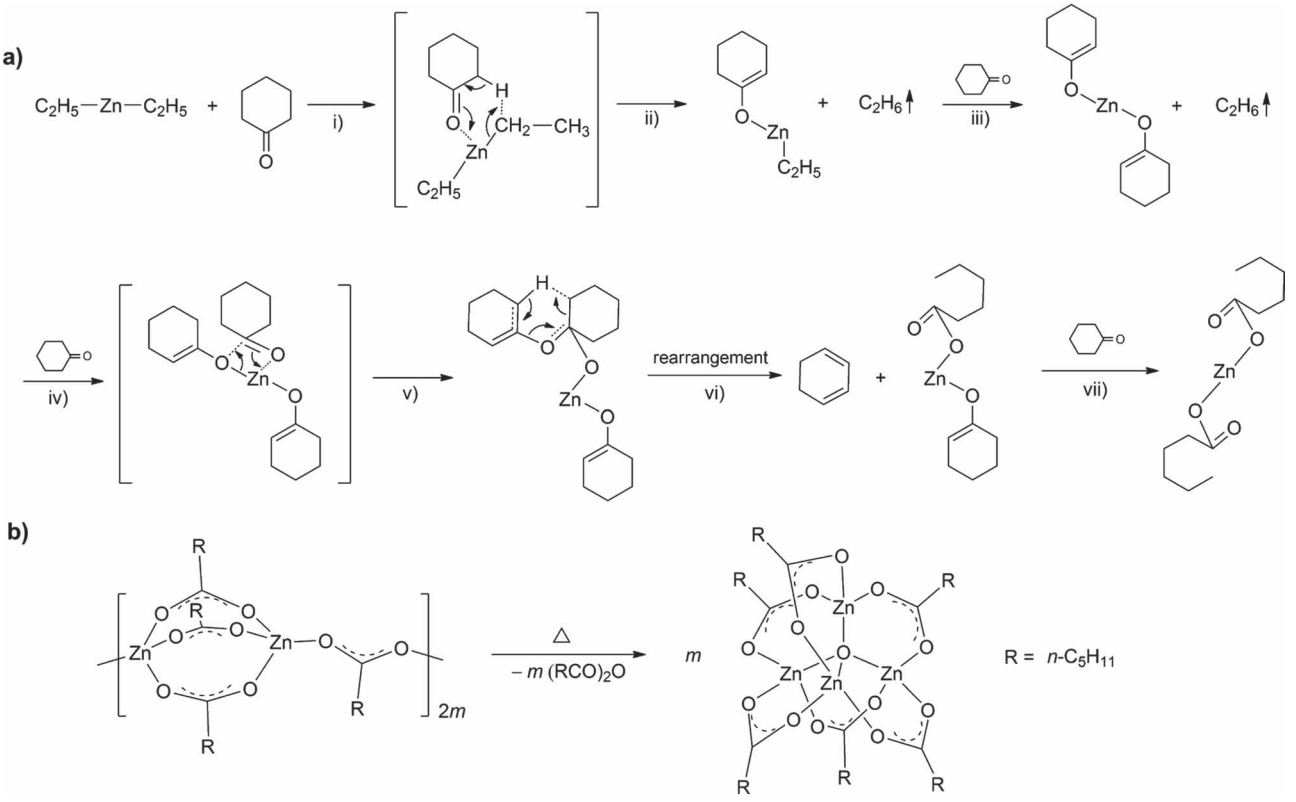

Scheme 2. Proposed reaction mechanisms for a) transformation of DEZn to zinc carboxylate in cyclohexanone solution and b) formation of zinc oxocarboxylates in the high-temperature annealed film.

at 1489 cm^{-1} similar as the dominant peaks in our 180 °C annealed film.[41] So we deduce that large amounts of zinc oxocarboxylates are formed in films annealed at higher temperatures such as 180 °C. Nuclear magnetic resonance (NMR) spectroscopy and pyrolysis gas chromatography mass spectrometry (GC/MS) have also been employed to validate the chemical structure of the organozinc compound (see Section S1 and S2 in Supporting Information).

Scheme 2 shows the possible mechanism for conversion of DEZn to zinc carboxylates with cyclohexanone as the solvent. The interaction of cyclohexanone and diethylzinc may take place at the carbonyl oxygen and at an active hydrogen simultaneously through a cyclic structure as suggested by Sakata et al. (step i in Scheme 2a).[42] Consequently, an ethylzinc alkoxide was formed by the hydrogen abstraction reaction (step ii in Scheme 2a). Such an ethylzinc alkoxide can further react with cyclohexanone to form a zinc dialkoxide through the same process as step i and ii (see step iii in Scheme 2a). The zinc dialkoxide is not stable and can react with cyclohexanone through an S_N2-type reaction (see step iv in Scheme 2a), which is similar with the reaction between zinc dialkoxides and epoxides.[23] Then the intermediate can be further converted to zinc monocarboxylate through step v and vi. The zinc monocarboxylate monoalkoxide will transform to zinc dicarboxylate by reacting with cyclohexanone (see step vii in Scheme 2a). The two carboxylic groups can act as ligands to form a stable organozinc compound. At lower temperatures such as RT, the organozinc compound existed in a form of linear chain polymer as verified by the IR spectra analyzed above. When annealed at a higher temperature (≥120 °C), this kind of linear chain polymer can be converted to zinc oxocarboxylates (Scheme 2b).[40] Such zinc oxocarboxylates are more feasible to crystallize than the linear polymer of zinc carboxylates. As a result, films annealed at higher temperatures (≥120 °C) show a sharp and intense crystalline peak at $2\theta = 32.8°$ in the XRD patterns. In the case of SAM-modified organozinc film, the IR spectrum shows a weakened peak at 1631 cm^{-1} but a strengthened one at 1531 cm^{-1} compared with the unmodified film annealed at 180 °C (Figure 3). This means the SAM modification can break the coordination bonds between zinc and carboxylate ligands. It in turn causes a molecular structure change in those zinc oxocarboxylate molecules exposed to SAM molecules.

Figure 4 shows the water contact angle measurements on the surfaces of SAM modified SiO_2, organozinc film annealed at 180 °C, and SAM modified 180 °C-annealed organozinc film. The OTMS modified SiO_2 surface shows a water contact angle of 105.4° similar to the value reported by others.[12] Without OTMS modification, the 180 °C-annealed organozinc film exhibits a low water contact angle of 92.3°. However, after surface modification by OTMS, the 180 °C-annealed organozinc film shows a water contact angle of 111.7° which is even higher than the value of OTMS-modified SiO_2. This result clearly verifies that the organozinc compound can interact with OTMS and form SAM on its surface. It should be noted that in most cases a dielectric surface

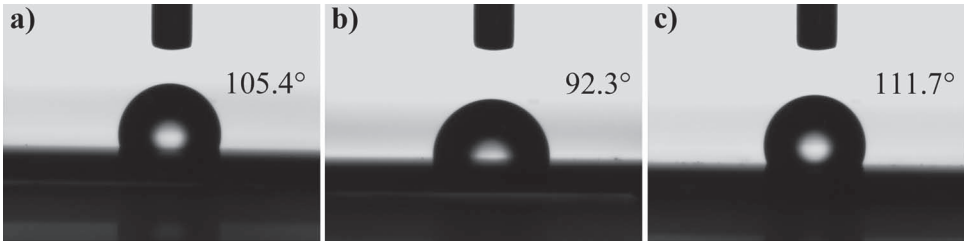

Figure 4. Water contact angles on surfaces of a) OTMS modified SiO_2, b) SiO_2 covered by organozinc film (annealed at 180 °C), and c) SiO_2 covered by OTMS modified organozinc film (annealed at 180 °C).

with higher water contact angle is beneficial to the orientation of semiconductor molecules and the morphology of semiconductor layers on it.[9] In addition, X-ray photoelectron spectroscopy (XPS) has been utilized to compare the surface coverage of the three dielectric modification layer (OTMS, organozinc film, and OTMS modified organozinc film) on SiO_2 (see details in Section S3 of Supporting Information). The XPS data also verify the successful assembly of OTMS on the organozinc film.

Figure 5 shows the morphology of SiO_2 dielectric layer after different modifications. The atomic force microscopy (AFM) images of OTMS modified SiO_2 exhibit an incontinuous coverage of SAM on the SiO_2 surface (see Figure 5a). Moreover, there are lots of small aggregates of the hydrolyzed OTMS molecules existed on the surface. The root mean square roughness (R_q) of this surface is 1.74 nm. When using organozinc compound as the modification layer on SiO_2 (annealed at 180 °C), the surface appears to be covered by nanoparticles with sizes ranging from 100 to 250 nm (Figure 5b). This surface is quite rough and shows an R_q value of 19.3 nm. However, after deposition of OTMS on the 180 °C-annealed organozinc layer and being treated by $NH_3 \cdot H_2O$ vapor for 3 hours, the size of organozinc nanoparticles becomes very small and the R_q value of the surface decreases to 0.60 nm (Figure 5c). With increasing the time of $NH_3 \cdot H_2O$ vapor treatment to 8 hours, on the surface of OMTS-modified organozinc layer most of the domains exhibit a smooth and continuous morphology except that some hills which are composed of hydrolyzed and polymerized OTMS come into being (Figure 5d). The smooth and continuous domain has a very small R_q value of 0.28 nm. Due to the existence of some hills, the whole image shows an R_q value of 1.11 nm. This means that the organozinc film undergoes a transformation from organozinc nanoparticles with bigger sizes to smaller ones and then to a smooth and continuous film during SAM modification. The reason may be that the hydrolyzed OTMS can react with organozinc compound by binding to it through Si-O-C or Si-O-Zn linkage and convert the crystalline zinc oxocarboxylates to amorphous chain polymers. With increasing the time of $NH_3 \cdot H_2O$ vapor treatment, more and more OTMS molecules are hydrolyzed leading to an enhanced conversion of zinc oxocarboxylates to chain polymers on the film surface. Since molecules stacked in an amorphous state are more easily to form good film than those in a crystalline state, smooth and continuous film morphology can thus be obtained for the organozinc layer treated by OTMS.

To evaluate the effect of surface modification on the performance of OFETs, devices with two configurations were fabricated, which employ the OTMS modified organozinc compound and the sole OTMS as the dielectric modification layer, respectively (see **Scheme 3**). Tens of devices were fabricated using each of the two configurations. **Figure 6** shows the representative device performance of the two configurations with poly(3-hexylthiophene) (P3HT) as the polymer semiconductor. Devices included in Figure 6 are labeled as device I (with the configuration in Scheme 3a) and II (with the configuration in Scheme 3b),

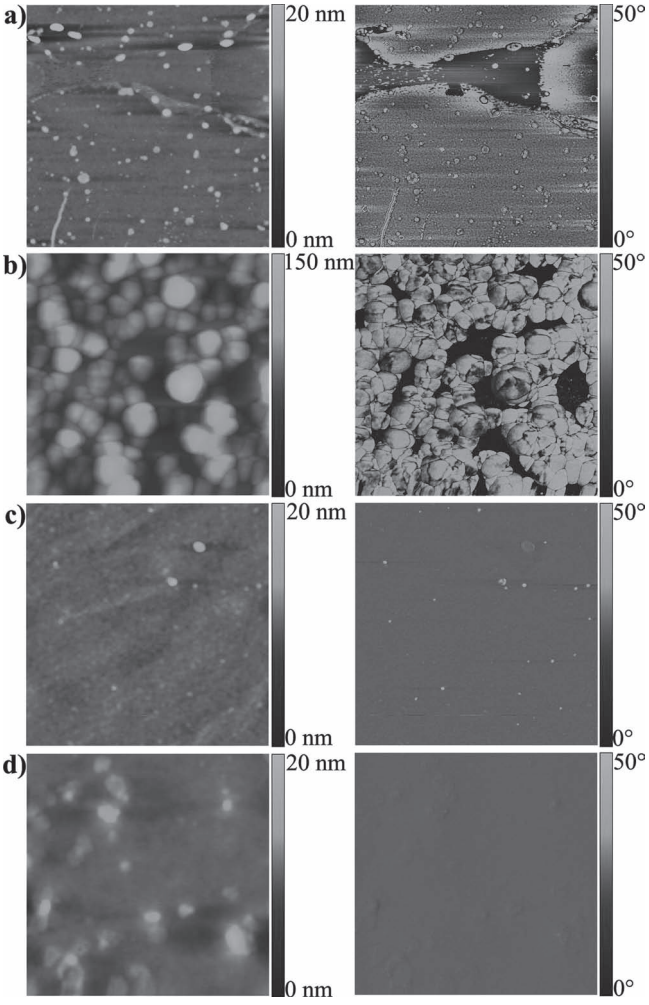

Figure 5. AFM images of the surface morphology of a) OTMS modified SiO_2, b) 180 °C-annealed organozinc film, and OTMS modified 180 °C-annealed organozinc film with $NH_3 \cdot H_2O$ vapor treatment for different time: c) 3 h and d) 8 h. The left and right panels show the height images and phase images, respectively, with a 2 μm × 2 μm scale.

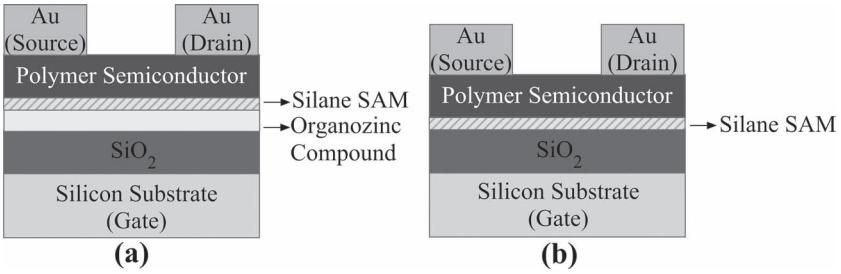

Scheme 3. Configurations of a) devices with organozinc compound as the dielectric modification layer and b) the control devices which do no comprise the organozinc layer.

respectively. From the output curves (Figure 6a,c) we can see, both the devices exhibit typical p-type FET behaviors working at an accumulation mode. It means the transporting carriers in the channel are holes. From the transfer curves (Figure 6b,d) we can calculate the field-effect mobility (μ) by using Equation (1) in the saturation regime:

$$I_{DS} = \frac{WC_i}{2L}\mu\,(V_G - V_T)^2 \quad (1)$$

where I_{DS} is the drain current, W and L are the channel width and length, respectively, C_i is the capacitance per unit area of the gate insulator, V_G is the gate voltage, and V_T is the threshold voltage. Device II shows a hole mobility of 7.55×10^{-2} cm^2 V^{-1} s^{-1} which approaches the optimum value for pure P3HT based OFETs.[43,44] Device I shows an enhanced hole mobility of 1.54×10^{-1} cm^2 V^{-1} s^{-1} which is about twice of that of device II. Both of the two devices have positive threshold voltages and their values are similar (20.0 V for device I and 20.8 V for device II). The positive threshold voltage originates from the trapped (immobile) negative charges in the dielectric layer.[45] The immobile negative charges may come from carboxylate ligand groups in organozinc layer for device I and from incompletely reacted SiOH groups of SiO_2 surface or hydrolyzed OTMS for device II.[16] Such immobile negative charges attracts and retains mobile holes in P3HT leading to a positive threshold voltage.

Since P3HT has a very good electron-donating ability, holes can easily be induced at the polymer semiconductor (P3HT)/dielectric interface by transferring electrons to the carboxylate ligand groups or SiOH groups in the dielectric layer, leaving the interface covered by holes (**Scheme 4**a). However, if the electron-donating ability of a polymer semiconductor is weaker, holes

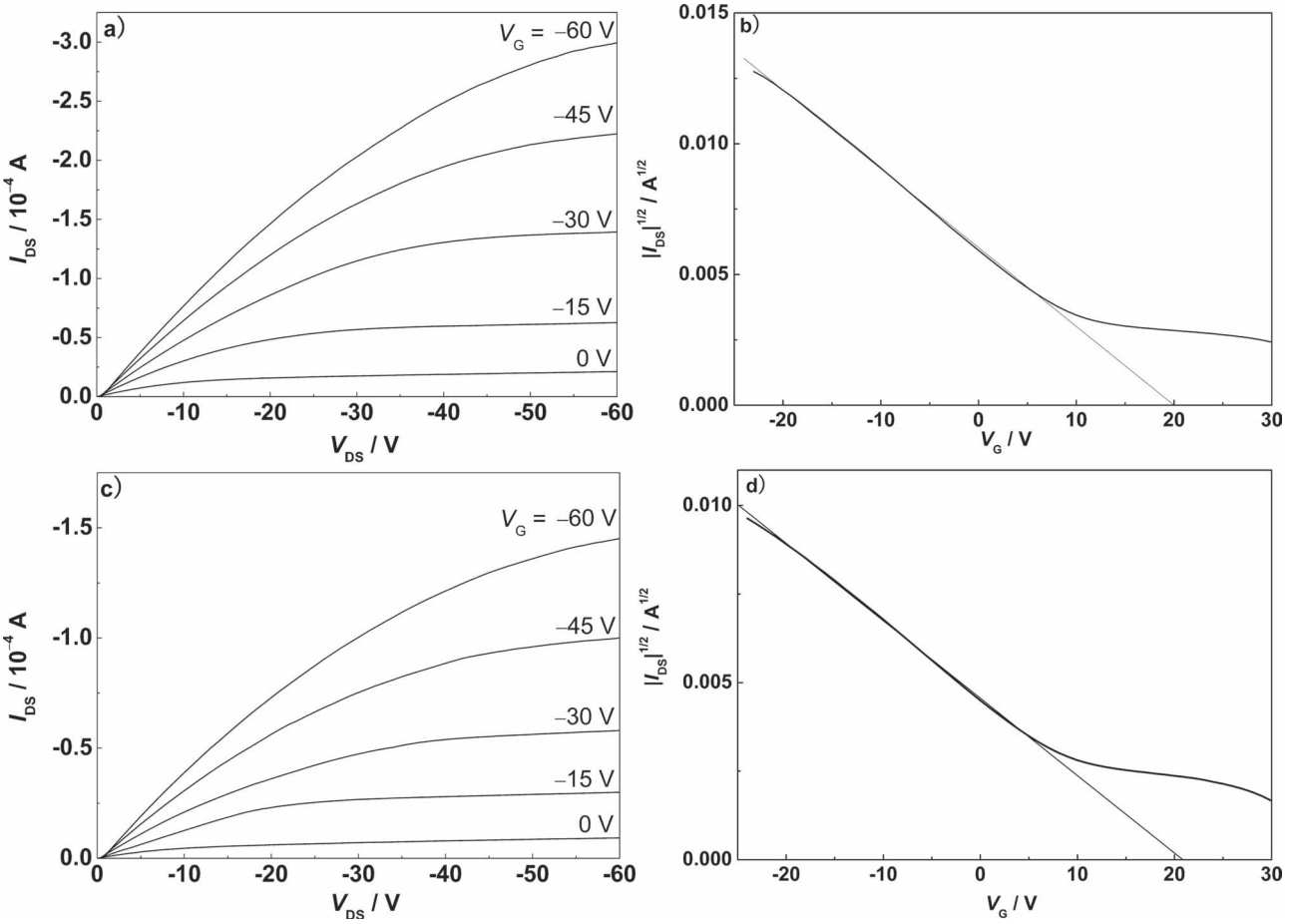

Figure 6. a) Output and b) transfer characteristics of P3HT-based FET containing the organozinc film (with the configuration in Scheme 3a) in comparison with c) output and d) transfer curves of the control device (with the configuration in Scheme 3b). The linear fit has also been shown in (b,d).

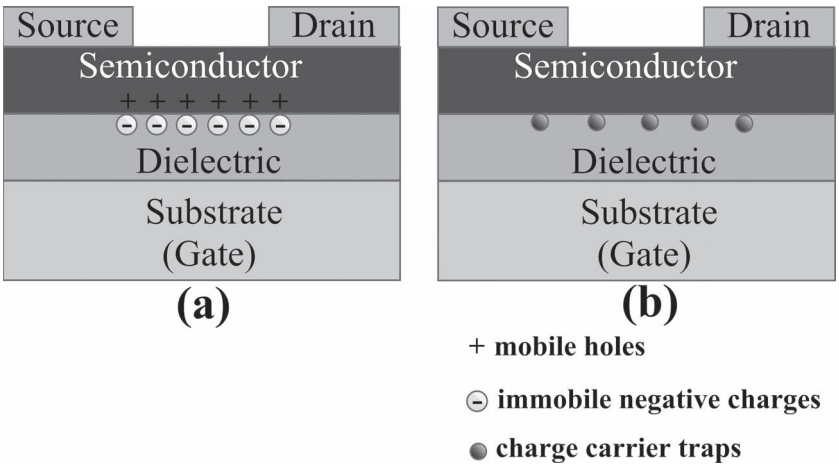

Scheme 4. Illustrations of the semiconductor/dielectric interface states in a p-type OFET with a) positive and b) negative threshold voltages.

can hardly be induced at the polymer semiconductor/dielectric interface. As a result, there are no retained holes at the interface when the electrodes are grounded. It is well known that in most cases there are some charge carrier traps existed at the interface between semiconductor and dielectric layers in OFETs (Scheme 4b).[9] So an additional negative gate voltage must be applied to induce holes from the p-type polymer semiconductor to fill charge traps at the interface, leading to a negative threshold voltage. OFETs with p-type polymers which exhibit either a positive V_T or a negative one are both widely reported.[46,47] The above results of device I and II have shown that OTMS modified organozinc compound works well as a dielectric modification layer for p-type OFETs with a positive V_T. To investigate the effect of organozinc dielectric modification layer on p-type OFETs with a negative V_T, we fabricated devices with the two configurations shown in Scheme 3 using a polymer semiconductor **P1** which contains 4,8-bis(2-ethylhexyloxy)benzo[1,2-b:4,5-b']dithiophene and 4,4'-dinonyl-2,2'-bithiazole as the repeating units. **P1** has an ionization potential of 5.1 eV which is larger than that of P3HT (4.7 – 4.9 eV).[48–50] So **P1** has a weaker electron donating ability than P3HT. **Figure 7** shows the representative device performance of the two configurations

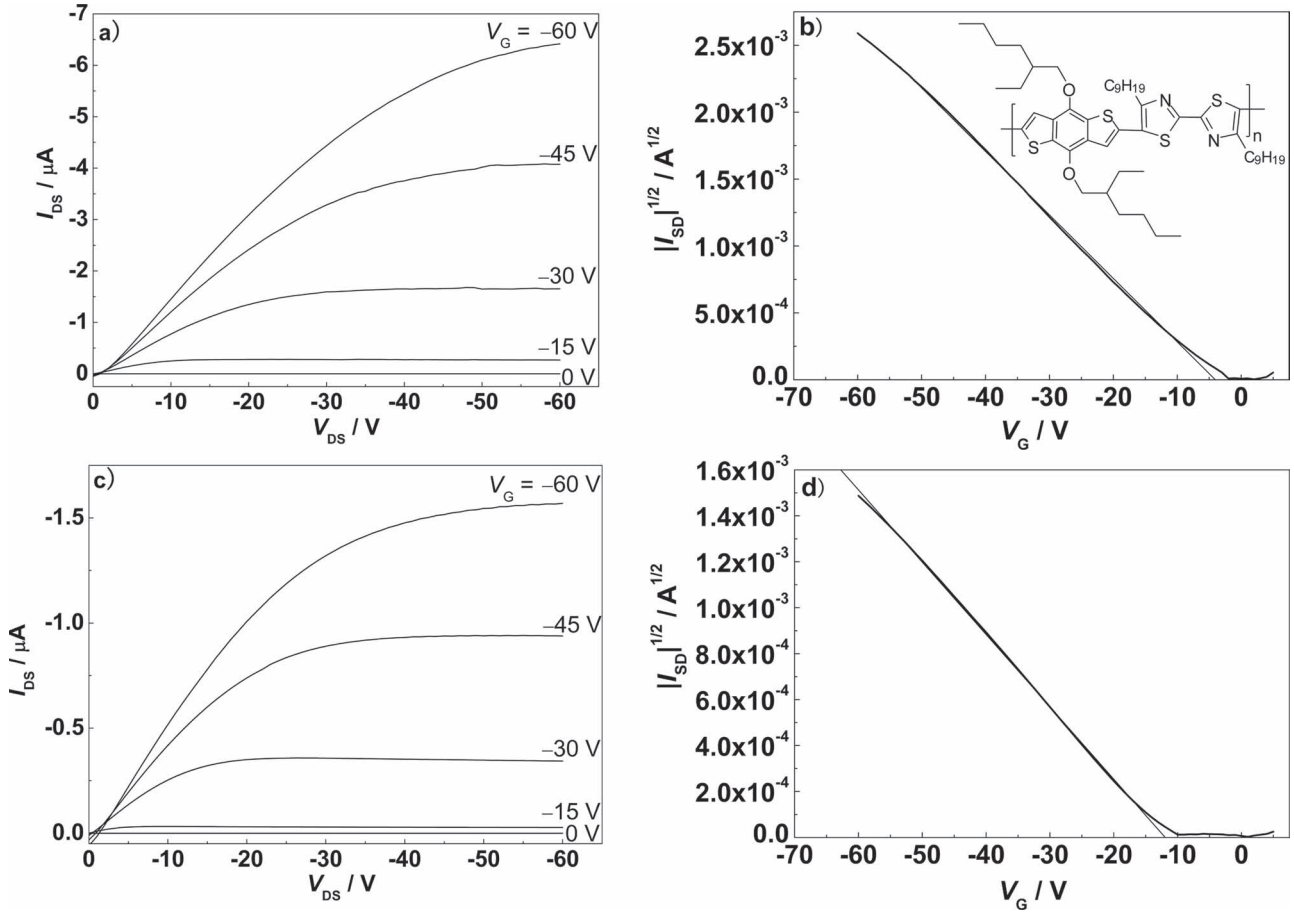

Figure 7. a) Output and b) transfer characteristics of **P1** based FET containing the organozinc film (with the configuration in Scheme 3a) in comparison with c) output and d) transfer curves of the control device (with the configuration in Scheme 3b). The inset in (b) is the chemical structure of **P1**. The linear fit has also been shown in (b,d).

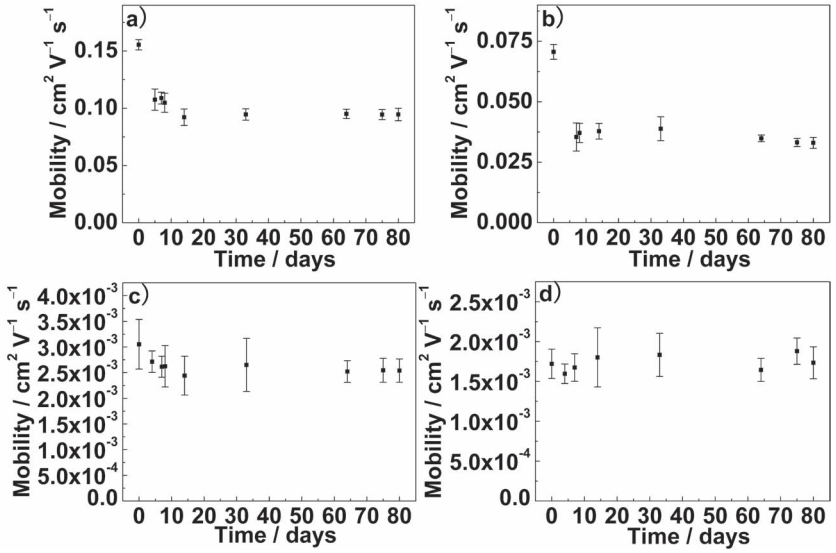

Figure 8. The stability of P3HT based FETs with the configuration in a) Scheme 3a and b) Scheme 3b and that of **P1** based FETs with the configuration in c) Scheme 3a and d) Scheme 3b. The statistics are based on nine devices for each kind of device structures.

with **P1** as the polymer semiconductor. Devices included in Figure 7 are labeled as device III (with the configuration in Scheme 3a) and IV (with the configuration in Scheme 3b), respectively. Device III shows a hole mobility of 3.69×10^{-3} cm^2 V^{-1} s^{-1} which is more than two-fold larger than that of device IV (1.57×10^{-3} cm^2 V^{-1} s^{-1}). Unlike P3HT based devices, both device III and IV, which employs **P1** as the polymer semiconductor, have a negative threshold voltage. Furthermore, they show an obvious difference in V_T which is –4 V for device III and –12 V for device IV. It is generally accepted that the value of $|V_T|$ is related with the number of charge traps at the interface of organic semiconductor/dielectric. Lower $|V_T|$ means less charge traps existed.[10] So it indicates that the dielectric modification layer in device III which is composed of OTMS modified organozinc compound has less charge traps than that in device IV with OTMS only. The reduced charge traps in OTMS modified organozinc compound layer may be attributed to improved surface morphology and SAM coverage as verified by AFM measurement and reduced surface polarity as proved by water contact angle test. The decrease in charge traps at the semiconductor/dielectric interface also facilitate the transport of charge carriers and lead to an increase in the hole mobility of devices with the OTMS modified organozinc compound layer relative to devices without organozinc compound.

The stability of these polymer FETs have been tested at ambient circumstance. As shown in **Figure 8**a,b, P3HT based devices both with and without organozinc dielectric modification layer show a fast drop of hole mobilities at the first few days. After that, the mobility tends to be unchanged for devices with organozinc compound but it still decreases with time for devices without organozinc compound. The hole mobility reaches 61% of its initial value for organozinc modified devices after 80 days and the percentage is 47% for the control devices. So the device stability has been improved for P3HT based FETs by introducing organozinc compound. With organozinc compound as the dielectric modification layer, **P1** based devices show a similar trend in the change of mobility value with time as P3HT based ones do (see Figure 8c). However, the control devices (**P1** based devices without organozinc modification) exhibit fluctuating mobility values with time (see Figure 8d), which may be caused by the unstable interface between polymer semiconductor and the dielectric.

Besides organozinc compound mentioned in this work, other materials which can increase the SAM coverage on dielectric layer also have the possibility to improve the carrier mobility in OFETs. To check this possibility, alternative method for increased SAM coverage has been explored. We choose titanium (diisopropoxide) bis(2,4-pentanedionate) (TIPD) as the dielectric modification material. TIPD can lose its isopropoxy groups and be converted to TOPD after thermal annealing.[51] Similar with the organozinc compound, TOPD can be modified with OTMS SAM and then exhibits a highly hydrophobic surface (see Section S4 in Supporting Information). However, both P3HT and **P1** based FETs using OTMS-TOPD as the dielectric modification layer show reduced carrier mobility than the control device (OTMS on bare SiO_2 as the dielectric layer) (see Section S5 in Supporting Information). The reason is still unclear now. One possible reason is that OTMS modified TOPD film does not improve the surface roughness (see Figure S6 in Supporting Information) while OTMS modified organozinc film can obviously improve the surface roughness.

3. Conclusions

We have utilized organozinc compound to act as an effective dielectric modification layer between SiO_2 and OTMS SAM in polymer FETs. Such an organozinc compound originates from the reaction between DEZn and cyclohexanone. At room temperature, the organozinc compound in films is composed of bridged zinc carboxylates in a chain polymer form. However, at a high annealing temperature such as 180 °C, the organozinc compound mainly exists in the form of zinc oxocarboxylates which is more crystalline than the chain polymer form. SAM of OTMS deposited onto the surface of the 180 °C annealed organozinc film shows improved surface morphology and reduced surface polarity compared with the one deposited onto bare SiO_2. Polymer FETs using the OTMS modified organozinc compound as a dielectric modification layer exhibit hole mobilities two-fold larger than those without the organozinc compound layer both for p-type polymer FETs with a positive threshold and with a negative one. In addition, employing the organozinc dielectric modification layer also helps reduce $|V_T|$ largely for p-type polymer FETs having a negative V_T value, benefited from decreased charge traps at the semiconductor/dielectric interface. Polymer FETs with such an organozinc compound layer

exhibit a good long-term stability which is better to the ones employing silane SAMs as the dielectric modification layer only. Organozinc compound has been employed as an interface modification layer in OFETs for the first time. We thus provide a new and effective method to improve the interfacial effect at the semiconductor/dielectric interface in OFETs.

4. Experimental Section

Materials and Instruments: P3HT (M_w = 30,000) with 98% regioregularity was purchased from Beijing Synwit Technology Co., Ltd. The polymer semiconductor **P1** was synthesized according to the reported process.[48] DEZn solution (1.0 M in heptane) and OTMS were purchased from Sigma-Aldrich Co. Cyclohexanone was obtained from Beijing Chemical Reagent Co. 75% TIPD isopropanol solution was purchased from Alfa Aesar Co. PL and UV-Vis spectra were collected with a Hitachi F-7000 fluorescence spectrophotometer and a Hitachi U-3900H spectrophotometer, respectively. XRD analysis was performed on a Rigaku D/Max-RB X-ray diffractometer using Cu Kα radiation. The IR transmission measurements were conducted on a Bio-RAD FTS-60V spectrometer using a reflection mode under vacuum conditions. Contact angle analyses were performed on an optical contact angle apparatus (OCA 20 DataPhysics Instruments GmbH, Germany) and the SCA20 software (Data Physics Instruments GmbH, Germany) was used for data acquisition. The AFM images were obtained from a Veeco DI Dimension V atomic force microscope operating in the tapping mode. The film thickness was measured by Ambios Technology XP-2 profilometer. The capacitances of dielectric layers were determined through AC impedance method using a CHI660 electrochemistry analyzer. The characteristics of OFETs were measured by a Keithley 4200 SCS semiconductor parameter analyzer under ambient conditions.

Preparation of the Organozinc Compound Films: DEZn solution (1.0 M in heptane, 0.2 mL) was injected into cyclohexanone (10 mL) and the obtained solution showed a light yellow color. Then this solution was filtered through a 0.45 μm polytetrafluoroethylene (PTFE) filter. Such a solution is very stable over several months with no evidence of aggregation and precipitation. Organozinc compound films were deposited from the above solution onto the surfaces of different substrates including quartz flakes (for PL and UV-Vis spectra measurement), single-crystal (100) silicon wafers (for XRD and IR spectra measurement), and thermally oxidized (100) silicon wafers (for contact angle, AFM measurements and OFET device fabrication). After solvent evaporation, these organozinc films were annealed at various temperatures (90, 120, and 180 °C) on a hotplate in air for 20 min.

Fabrication of Polymer FETs: Thermally oxidized (100) silicon wafers (n^{++} doped) with a SiO_2 thickness of 300 nm were sequentially cleaned with detergent, deionized water, acetone and ethanol in ultrasonic bath. Then hydrophilic treatment of these silicon wafers was performed according to the standard procedure. Briefly, the substrates were soaked in a mixture of deionized water, 25% ammonium hydroxide and 30% H_2O_2 (5:1:1 by volumetric ratio) for 20 min at 80 °C, then rinsed with deionized water and dried with nitrogen flow. The organozinc film was spin-coated onto the surface of hydrophilic-treated SiO_2 dielectric layer to give a thickness of 30 nm. Then the organozinc film was annealed at 180 °C on a hotplate for 20 min. Deposition of OTMS SAM both on 180 °C-annealed organozinc film and on bare SiO_2 surface was similar to the reported method,[12] except that more dilute ammonium hydroxide solution (5% in water) for vapor annealing of the SAM and reduced time (8 h) were used in our experiment. Then the substrates were rinsed by heptane to remove the physically adsorbed OTMS molecules. P3HT film was deposited from its chlorobenzene solution by spin-coating to give a thickness of 90 nm. Before spin-coating, the P3HT chlorobenzene solution was let to stand on the dielectric modification layer for 10 min for better wetting of the surface. **P1** film was deposited from its chloroform solution onto the surface of the dielectric modification layer without prewetting and the film thickness is 50 nm. Both of the P3HT and P1 films were annealed at 180 °C for 15 min in a vacuum oven under a pressure less than 1.3 mbar. Finally, Au source and drain electrodes were deposited on the polymer semiconductor layer through vacuum thermal evaporation. The channel width and channel length are 8800 μm and 80 μm, respectively. The capacitance per unit area (C_i) of OTMS modified SiO_2 is 11.5 nF cm^{-2} and the one of OTMS-organozinc compound modified SiO_2 is 11.1 nF cm^{-2}, which were obtained by AC impedance measurement.

Supporting Information

Supporting Information is available from the Wiley Online Library or from the author.

Acknowledgements

This work is supported by the National Natural Science Foundation of China (90923015, 50803006), National Laboratory for Molecular Sciences, the Program for Changjiang Scholars and Innovative Research Team in University and the Fundamental Research Funds for the Central Universities of China.

Received: February 2, 2012
Revised: May 16, 2012
Published online: June 13, 2012

[1] D. Voss, *Nature* **2000**, *407*, 442.
[2] P. F. Baude, D. A. Ender, M. A. Haase, T. W. Kelley, D. V. Muyres, S. D. Theiss, *Appl. Phys. Lett.* **2003**, *82*, 3964.
[3] J. A. Rogers, Z. Bao, K. Baldwin, A. Dodabalapur, B. Crone, V. R. Raju, V. Kuck, H. Katz, K. Amundson, J. Ewing, P. Drzaic, *Proc. Natl. Acad. Sci. USA* **2001**, *98*, 4835.
[4] L. Torsi, A. Dodabalapur, *Anal. Chem.* **2005**, *77*, 380 A.
[5] A. R. Murphy, J. M. J. Frechet, *Chem. Rev.* **2007**, *107*, 1066.
[6] A. Ruiz, A. Papadimitratos, A. C. Mayer, G. G. Malliaras, *Adv. Mater.* **2005**, *17*, 1795.
[7] F. Dinelli, M. Murgia, P. Levy, M. Cavallini, F. Biscarini, D. M. de Leeuw, *Phys. Rev. Lett.* **2004**, *92*, 116802.
[8] C. Di, Y. Liu, G. Yu, D. Zhu, *Acc. Chem. Res.* **2009**, *42*, 1573.
[9] X. Sun, C. Di, Y. Liu, *J. Mater. Chem.* **2010**, *20*, 2599.
[10] L. Miozzo, A. Yassar, G. Horowitz, *J. Mater. Chem.* **2010**, *20*, 2513.
[11] H. Ma, H.-L. Yip, F. Huang, A. K. Y. Jen, *Adv. Funct. Mater.* **2010**, *20*, 1371.
[12] Y. Ito, A. A. Virkar, S. Mannsfeld, J. H. Oh, M. Toney, J. Locklin, Z. Bao, *J. Am. Chem. Soc.* **2009**, *131*, 9396.
[13] A. Virkar, S. Mannsfeld, J. H. Oh, M. F. Toney, Y. H. Tan, G. Liu, J. C. Scott, R. Miller, Z. Bao, *Adv. Funct. Mater.* **2009**, *19*, 1962.
[14] E. L. Hanson, J. Schwartz, B. Nickel, N. Koch, M. F. Danisman, *J. Am. Chem. Soc.* **2003**, *125*, 16074.
[15] O. Acton, D. Hutchins, L. Árnadóttir, T. Weidner, N. Cernetic, G. G. Ting, T.-W. Kim, D. G. Castner, H. Ma, A. K.-Y. Jen, *Adv. Mater.* **2011**, *23*, 1899.
[16] L.-L. Chua, J. Zaumseil1, J.-F. Chang, E. C.-W. Ou, P. K.-H. Ho, H. Sirringhaus, R. H. Friend, *Nature* **2005**, *434*, 194.
[17] L.-L. Chua, P. K. H. Ho, H. Sirringhaus, R. H. Friend, *Appl. Phys. Lett.* **2004**, *84*, 3400.
[18] X. Cheng, M. Caironi, Y.-Y. Noh, J. Wang, C. Newman, H. Yan, A. Facchetti, H. Sirringhaus, *Chem. Mater.* **2010**, *22*, 1559.
[19] T. Nagase, T. Hamada, K. Tomatsu, S. Yamazaki, T. Kobayashi, S. Murakami, K. Matsukawa, H. Naito, *Adv. Mater.* **2010**, *22*, 4706.
[20] Y. Wu, P. Liu, B. S. Ong, *Appl. Phys. Lett.* **2006**, *89*, 013505.

[21] A. A. Virkar, S. C. B. Mannsfeld, Z. Bao, *J. Mater. Chem.* **2010**, *20*, 2664.
[22] M. Ishimori, T. Tsuruta, *Makromol.* **1963**, *64*, 190.
[23] M. Ishimori, O. Nakasugi, N. Takeda, T. Tsuruta, *Makromol.* **1968**, *115*, 103.
[24] Š. Vyskočil, S. Jaracz, M. Smrčina, M. Štícha, V. Hanuš, M. Polášek, P. Kočovský, *J. Org. Chem.* **1998**, *63*, 7727.
[25] K. Yearick, C. Wolf, *Org. Lett.* **2008**, *10*, 3915.
[26] A. P. Duncan, J. L. Leighton, *Org. Lett.* **2004**, *6*, 4117.
[27] C. Bárcena, A. K. Sra, G. S. Chaubey, C. Khemtong, J. P. Liu, J. Gao, *Chem. Commun.* **2008**, 2224.
[28] C. Gutsche, I. Regolin, K. Blekker, A. Lysov, W. Prost, F. J. Tegude, *J. Appl. Phys.* **2009**, *105*, 024305.
[29] R. E. Algra, M. A. Verheijen, M. T. Borgström, L.-F. Feiner, G. Immink, W. J. P. van Enckevort, E. Vlieg, E. P. A. M. Bakkers, *Nature* **2008**, *456*, 369.
[30] W. J. E. Beek, L. H. Sloof, M. M. Wienk, J. M. Kroon, R. A. J. Janssen, *Adv. Funct. Mater.* **2005**, *15*, 1703.
[31] D. J. D. Moet, L. J. A. Koster, B. de Boer, P. W. M. Blom, *Chem. Mater.* **2007**, *19*, 5856.
[32] S. D. Oosterhout, M. M.Wienk1, S. S. van Bavel, R. Thiedmann, L. J. A. Koster, J. Gilot, J. Loos, V. Schmidt, R. A. J. Janssen, *Nat. Mater.* **2009**, *8*, 818.
[33] E. A. Meulenkamp, *J. Phys. Chem. B* **1998**, *102*, 5566.
[34] S.-H. Choi, E.-G. Kim, J. Park, K. An, N. Lee, S. C. Kim, T. Hyeon, *J. Phys. Chem. B* **2005**, *109*, 14792.
[35] L. Dai, X. L. Chen, W. J. Wang, T. Zhou, B. Q. Hu, *J. Phys.: Condens. Matter* **2003**, *15*, 2221.
[36] W. Clegg, D. R. Harbron, C. D. Homan, P. A. Hunt, I. R. Little, B. P. Straughan, *Inorg. Chim. Acta* **1991**, *186*, 51.
[37] Y. Nakacho, T. Misawa, T. Fujiwara, A. Wakahara, K.-I. Tomita, *Bull. Chem. Soc. Jpn.* **1976**, *49*, 58.
[38] V. Zeleňák, Z. Vargová, K. Györyová, *Spectrochim. Acta Part A* **2007**, *66*, 262.
[39] E. G. Palaciosa, G. Juárez-Lópeza, A. J. Monhemius, *Hydrometallurgy* **2004**, *72*, 139.
[40] J. A. Andor, O. Berkesi, I. Dreveni, E. Varga, *Lubr. Sci.* **1999**, *11*, 115.
[41] K. Nakamoto, Y. Morimoto, A. E. Martell, *J. Am. Chem. Soc.* **1961**, *83*, 4528.
[42] R. Sakata, K. Takeuchi, H. Yoshii, K. Haga, A. Onishi, *Makromol.* **1966**, *98*, 253.
[43] H. Sirringhaus, P. J. Brown, R. H. Friend, M. M. Nielsen, K. Bechgaard, B. M. W. Langeveld-Voss, A. J. H. Spiering, R. A. J. Janssen, E. W. Meijer, P. Herwig, D. M. de Leeuw, *Nature* **1999**, *401*, 685.
[44] K. Sethuraman, S. Ochiai, K. Kojima, T. Mizutani, *Appl. Phys. Lett.* **2008**, *92*, 183302.
[45] S. G. J. Mathijssen, M.-J. Spijkman, A.-M. Andringa, P. A. van Hal, I. McCulloch, M. Kemerink, R. A. J. Janssen, D. M. de Leeuw, *Adv. Mater.* **2010**, *22*, 5105.
[46] J. Matsui, S. Yoshida, T. Mikayama, A. Aoki, T. Miyashita, *Langmuir* **2005**, *21*, 5343.
[47] J. S. Ha, K. H. Kim, D. H. Choi, *J. Am. Chem. Soc.* **2011**, *133*, 10364.
[48] M. Yang, B. Peng, B. Liu, Y. Zou, K. Zhou, Y. He, C. Pan, Y. Li, *J. Phys. Chem. C* **2010**, *114*, 17989.
[49] A. J. Cascio, J. E. Lyon, M. M. Beerbom, R. Schlaf, Y. Zhu, S. A. Jenekhe, *Appl. Phys. Lett.* **2006**, *88*, 062104.
[50] P. Ravirajan, A. M. Peiró, M. K. Nazeeruddin, M. Graetzel, D. D. C. Bradley, J. R. Durrant, J. Nelson, *J. Phys. Chem. B* **2006**, *110*, 7635.
[51] Z. Tan, W. Zhang, Z. Zhang, D. Qian, Y. Huang, J. Hou, Y. Li, *Adv. Mater.* **2012**, *24*, 1476.